SUBCONTRACT TITLE**:** **Fabrication and Physics of CdTe Devices by Sputtering**

SUBCONTRACT TITLE**:** **ZXL-5-44205-01**

QUARTERLY TECHNICAL STATUS REPORT FOR**:**

Phase 3/Quarter 4

SUBMITTED TO**:** **Bolko von Roedern**
National Renewable Energy Laboratory

PRINCIPAL INVESTIGATORS:

A.D. Compaan (P.I.), R.W. Collins, V.G. Karpov
Department of Physics and Astronomy
Dean Giolando, Dept. of Chemistry
The University of Toledo
Toledo, OH 43606

This technical progress report covers the Fourth Quarter of the extended Phase 3 for the period from April 1, 2008, through July 31, 2008, of the above Thin Film Photovoltaic Partnership Program subcontract.

This report presents results from a light-soaking study on magnetron-sputtered cells with approximately constant CdTe thickness and seven CdS thicknesses from 230 nm to 0 nm. Two sets of substrates were used--standard Pilkington TEC 15 and an HRT-coated TEC 15. A second study held the CdS thickness at 130 nm and varied the CdTe thickness from 0.3 μm to 2.25 μm. This study used only TEC 7 substrates. Light soaking was done in Toledo summer indoor air at one sun and open circuit.

In addition, the dielectric functions of CdTe and CdS have been modeled using the critical point (CP) parabolic band approximation. Key characteristics can be deduced including grain size, excitation group speeds, stress, and temperature from the CP parameters. Capabilities for on-line optical monitoring have been developed to provide information, not only on layer thicknesses and compositions, but also on grain size, stress, and temperature.

1 Light-soaking Study on Cells with Various CdS and CdTe Thickness

1.1 Introduction

In our Phase I Annual Report, we reported the fabrication of cells with ultra-thin CdTe layers down to 0.45μm with a best efficiency of 8%. Further optimization of the CdS thickness, $CdCl_2$ treatment, Cu thickness and back-contact activation time was reported in the third quarter of Phase III. In this current quarter, we studied the stability of the ultra-thin cells with various CdS and CdTe thicknesses under one-sun light soak (LS).

All the samples investigated in this studied were light-soaked in an Atlas SUNTEST XLS+ light stress system. Samples were light-soaked at open circuit at ~1800 W/m^2 illumination from an unfiltered Xe arc lamp. The sample temperature was controlled at 65 ^oC by flushing with heated room air. Samples were not encapsulated during light-soaking. The relative humidity was about 60% for the starting indoor air at 75 ^oF..

1.2 Cell Performance and Stability vs. CdS Thickness

For this set of samples, CdS and CdTe films were sputter-deposited on TEC 15 glass and on TEC 15 glass coated with a highly resistive transparent (HRT) layer. The sputtering was done at a substrate temperature of 250 ^oC with the two types of substrates mounted side-by-side (each 3.0 × 1.5 inch). Seven CdS layer thicknesses were chosen 0, 30, 45, 80, 130, 160 and 230 nm, while the CdTe layers were kept around our standard thickness but varied from 2.2-2.6 μm. Following deposition, a 30-minute vapor-$CdCl_2$ treatment was done at 387 ^oC simultaneously on the two types of substrates for each film thickness. The 3 nm Cu / 20 nm Au back contacts were deposited by evaporation and finally the Cu was diffused for 45 minutes at 150 ^oC. These samples were light soaked in the SUNTEST XLS+ system for a total 300 hours with all cells being removed and J-V tested after light soak durations of 1, 3, 10, 30, 100, and 300 hours. Ten cells of each CdS thickness were measured during light-soaking. Each CdS thickness set was divided into two sets with one of them light-soaked and the other one stored in the dark in room air to be used as reference cells.

1.2.1 Effect of Front Buffer Layer on Initial Performance

We found that cells on HRT-coated glass are less dependent on CdS layer thicknesses. As shown in Figure 1a, the average efficiencies of cells on HRT-coated substrates distribute in a narrow range between 9.8 and 11% before light soaking, for CdS thickness between 30 and 230 nm. The initial efficiencies of cells on TEC 15 glass without HRT are relatively lower and distribute more widely, between 7 and 10.2%. Such tendency remains after light soaking, although the distribution broadens for both substrates.

As shown in Figure 1c, before the LS, the V_{OC} of cells on the HRT-coated substrate are all between 750 and 800 mV nearly independent of CdS thickness, except for the CdS-free one. Reducing the CdS thickness can provide higher J_{SC} due to less light absorption in the CdS. However, thin CdS can lead to a V_{OC} loss; the V_{OC} on substrates without HRT decreases from 800 mV to 460 mV with decreasing CdS thickness. The HRT layer helps to prevent this effect and maintain a high V_{OC} even for a 30 nm CdS layer. A similar effect of the HRT on fill factor is also observed (not shown).

1.2.2 Effect of Front Buffer Layer on Stability

Even though the HRT layer yields high performance for thinner CdS cells, we do not observe any advantage in improving the stability of thin CdS cells. The average efficiencies of the seven different CdS thickness before and during the 300 hours of light soaking on TEC15 and HRT+TEC15 are shown in Figure 1b and 1a, respectively. For cells on HRT glass, degradation starts after 3 to 10 hours of light soaking. Cells on TEC 15 glass begin significant degradation after about 10 hours too but with a relatively slower rate. However, the initial efficiencies are somewhat lower so that the final efficiencies (at 300 hrs) of the cells on HRT-coated TEC 15 are still higher than that of the bare TEC 15 cells.

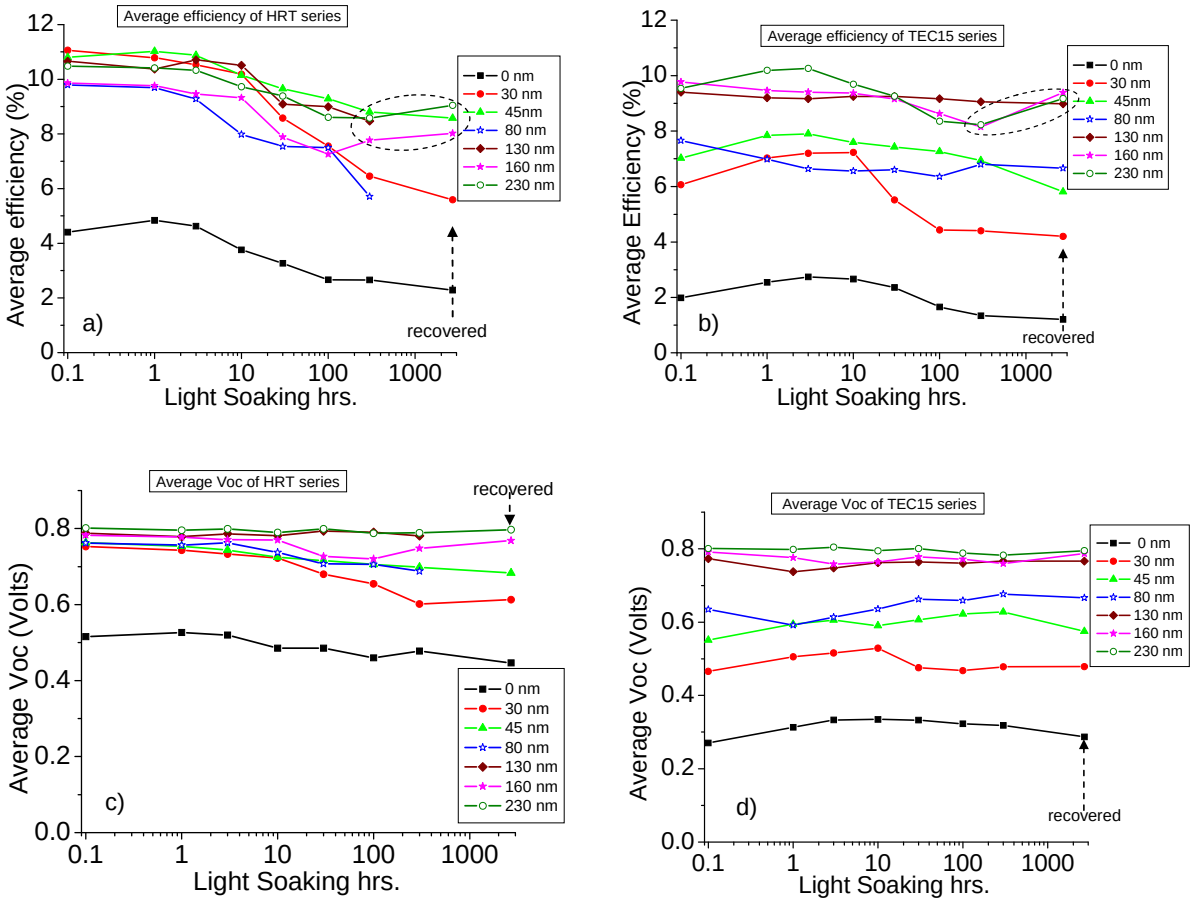

Figure 1 Ten-cell average efficiencies with different CdS thickness before and (periodically measured) during the light soaking together with recovery after 100 days plotted in a) for HRT and b) for TEC15 glass. The corresponding V_{OC} of HRT and TEC15 glass are plotted respectively in c) and d). For convenience, the initial performance measured just before the start of light soaking was plotted at 0.1 hrs.

Although the initial V_{OC} of cells on HRT glass is nearly independent of the CdS layer thickness for CdS ≥30 nm, V_{OC} starts decreasing after 10 hours of light-soaking for CdS less than 80 nm but remains almost constant for thicker CdS samples. The rate of decrease of V_{OC} for the thinnest CdS samples of 30 nm is the largest among all the samples. Cells without any CdS are more stable than the ones with 30nm CdS but the initial V_{OC} is much less. As expected, the J_{SC} increases with decreasing CdS for both substrates, and no dependence on substrate type is observed. (Data not shown.)

To display more clearly the degradation rate dependence on CdS thickness, we plot the ratio of final to initial efficiencies in Figure 2. It is readily noticed that cells on TEC 15 are generally more stable than the ones on HRT coated TEC 15, which is mostly due to lower initial efficiencies on substrates without HRT.

A clear dependence of degradation rate on CdS thickness has not been observed in this study.

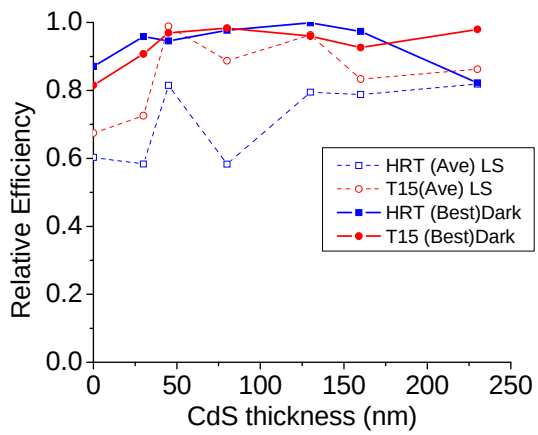

Figure 2. Ratios of cell efficiencies after to before light-soaking.

It is also worth noting that we are able to fabricate functioning cells without a CdS layer on both types of glass substrates. However, cells without CdS on HRT-coated glass yield an efficiency of 4.5%, while ones on TEC 15 yield only 2%. The V_{OC} of these CdS-free cells on HRT-coated glass is 516 mV compared with a V_{OC} of 270 mV on TEC 15.

1.2.3 Effect of Front Buffer Layer on Performance Recovery in Dark Storage

The last data points of Fig 2a and Fig. 2b show the cell performance recovery of samples which were stored in the dark at room temperature for 100 days after LS was finished. Cells with 160 nm and 230 nm of CdS show considerable recovery. This post-light-soak recovery apparently has a significant dependence on CdS thickness and is being studied further.

After the 300 hours light-soaking, these two sets of samples were stored in the dark and in ambient air at room temperature. After 100 days of storage, the cell performance was measured again. The relative changes of efficiencies are shown as the ratio of $Eff_{recovery}$ / $Eff_{stressed}$ and are plotted vs. CdS thickness in Figure 3.

As shown in Figure 3 and Figure 2a and 2b, only samples with CdS thicker than 130 nm exhibit efficiency recovery (ratio > 1) during the dark storage period, on either HRT or TEC15 substrates.

Samples with CdS between 80 and 130 nm retain their performance (ratio ≈1) at the end of light-soaking. Cells with CdS layers thinner than 80 nm appear to show further deterioration even in the dark.

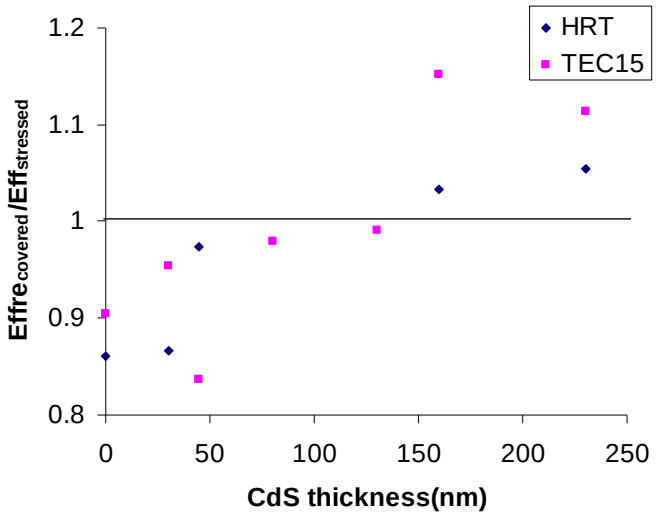

Figure 3 Ratios of average cell efficiencies after 100 days of dark storage ($Eff_{recovery}$) to efficiencies at the end of 300 hours of light-soaking at V_{OC} ($Eff_{stressed}$).

1.3 Cell performance and stability with Various CdTe thickness

Light soaking of cells with various CdTe layer thicknesses was also studied under the same light soak conditions for 1000 hours. CdS and CdTe films were sputtered on Pilkington TEC 7 glass substrate. (No substrates with HRT layers were used in this study.) The thickness of sputtered CdTe was varied from 0.3 to 2.25 μm with constant CdS thickness of 130 nm for each cell. (Based on the study of CdS thickness reported above, we anticipate that the use of an HRT coating would not substantially influence these data on CdTe thickness as long as the CdS thickness is 130nm or above.) In this series, the cells were wet-$CdCl_2$ treated at 387 ^{o}C for different durations, as opposed to the vapor $CdCl_2$-treatment of the previous study. The treatment times were chosen empirically as a linear function of CdTe thickness, which generated best performance for each CdTe thickness according to our previous study as reported for Phase 3, Quarter 3. A more detailed study of the relationship between treatment time and CdTe thickness is in progress and will be reported in the final technical report.

The $CdCl_2$ activation time as well as the Cu/Au back contact thickness and its activation time are shown in Table 1. A total of 35 cells of each CdTe thickness were measured during light-soaking. Another set of sample cells prepared under similar conditions were kept at room temperature in air to serve as references.

Remarkably, the cell stability appears to be independent of CdTe thickness over the full range from our standard 2.3 μm to as low as 0.3 μm after 1000 hrs of LS (Figure 4). More than 90% of the cells still have 80% of initial performance after 1000 hrs of light soaking. The ratios of average efficiencies after LS to those before LS are above 70% for all CdTe thicknesses. (See Fig. 4c.)

We find comparable performance of cells with CdTe thickness above 1.0 μm before and after the light-soaking. The initial average efficiencies of cells with 1.0, 1.32 and 2.25 μm CdTe are all

approximately between 9 and 10% which degrade to 8-9% after 1000 hours of LS. For the best cells, there is only 0.5% efficiency difference between 1.0 and 2.25 μm CdTe before LS.

Table 1. Cell fabrication parameters.

Sample IDs	CdTe (μm)	CdS (nm)	$CdCl_2$ (min.)	Cu/Au (nm)	diffusion time (min.)
SSC780A2	0.3	130	1	0.7/20	4
SSC782A1	0.5	130	3	0.9/20	5
SSC666A1	0.75	130	5	1.2/20	10
SSC652A1	1	130	10	1.7/20	15
SSC665A1	1.32	130	15	2.4/20	25
SSC718A2	2.25	130	25	3.3/20	45

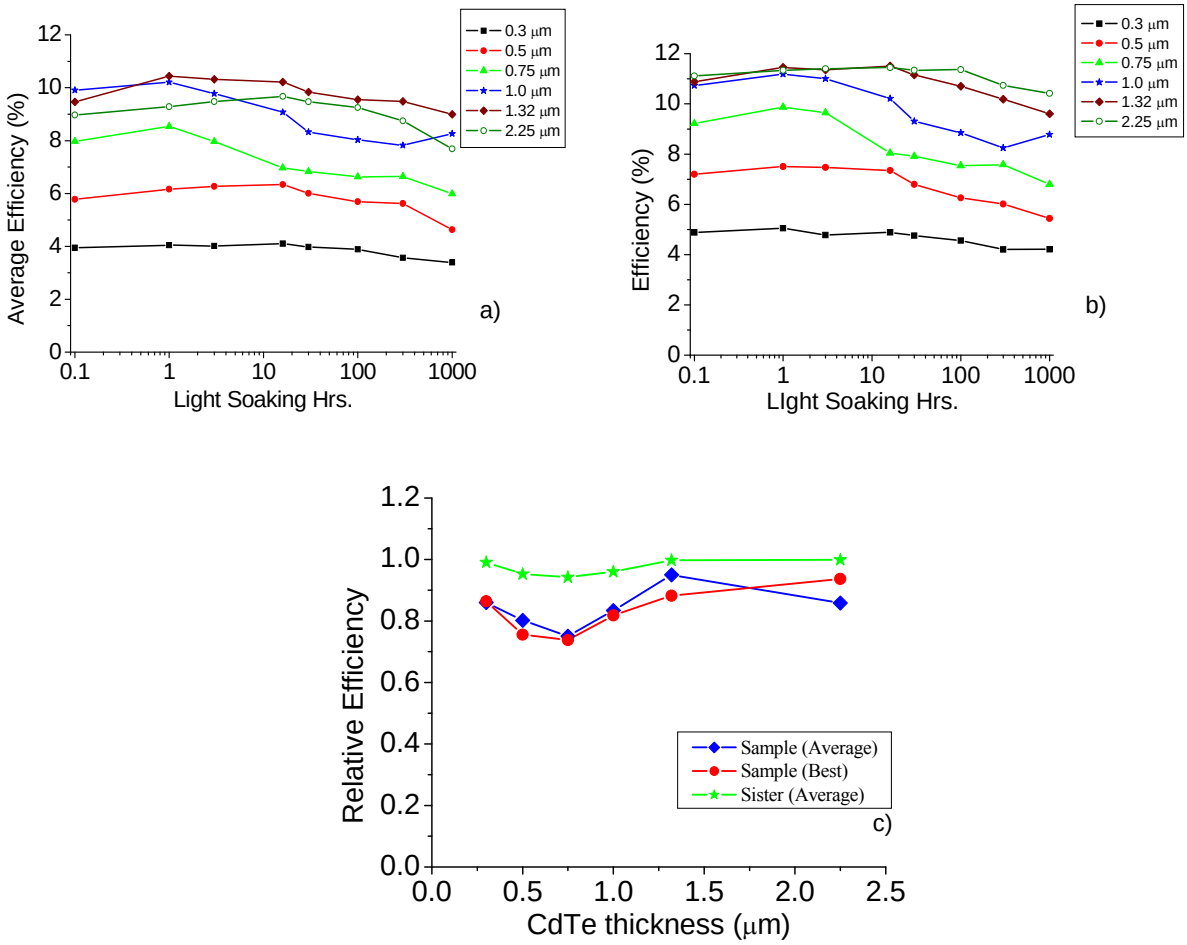

Figure 4 Average (a) and best cell (b) efficiencies vs. CdTe thickness on TEC 7 / 0.13μm CdS during 1000 hours of open-circuit light soaking. c) Ratios of cell efficiencies after LS to before LS.

Increase of series resistance is the major source of performance deterioration which reduces FF and V_{OC}. This may suggest degradation of the back contact. J_{SC} remains almost same during the

stressed period. The result also shows a general trend of somewhat better stability for thicker CdTe. However, the largest deterioration rate occurs at 0.75μm CdTe which is poorer than thinner CdTe cells, as shown in Figure 4c. However, this is somewhat misleading because of the much lower initial efficiencies of the thinner CdTe cells (Figure 4a and 4b).

1.4 Conclusions

HRT layers help produce high initial performance and uniformity of cells by maintaining high V_{OC} for thin CdS layers. However, no evidence appeared to indicate that the HRT layer improves the stability of sputtered cells under one-sun light soak at open circuit and no encapsulation. Cell degradation under light soak at open circuit occurs for cells on both HRT-coated TEC 15 glass and bare TEC15 glass, with somewhat greater degradation on HRT largely correlated with higher efficiency starting values.

Following 300 hours of light soak, cell performance recovery under dark storage for 100 days is found to be dependent on the CdS thickness. The thicker the CdS layer, the more the relative recovery. Reduced thickness of the CdS layer leads to greater loss of V_{OC} under light-stressed conditions for HRT substrates and less recovery in dark storage following light soak.

For cells with thinner CdTe layers on standard 130 nm CdS on bare TEC 7 glass, the performance stability does not get worse as CdTe gets thinner. The performance of cells with CdTe as thin as 1.0 μm is found to be equally stable to that from standard 2.25 μm CdTe. A study of thin CdTe cells on HRT-coated TEC glass is being carried out in order to understand the effect of HRT on the stability of ultra-thin CdTe cells.

Samples prepared for this study were all light-soaked without encapsulation and high relative humidity (Toledo summertime air with standard air conditioning). We are building a sealed chamber for further light-soaking studies to determine stability when cells are not exposed to water vapor and oxygen.

2. Optical Properties of CdTe and CdS

2.1 Introduction

The work reported here is a continuation of our efforts to develop the capabilities for on-line optical monitoring of the CdS and CdTe layers of solar cells (see: *Annual Technical Report for the Period of June 1, 2006 to May 31, 2007, Contract No. RXL-5-44205-01*). Previously we reported: (1) variations of E_0 and Γ_0 for CdTe and CdS films as approximately linear functions of measurement temperature T_m with temperature coefficients C_{TE} and $C_{T\Gamma}$, respectively; (2) variations of the broadening parameters Γ_n of CdTe and CdS films for all major critical points (CPs) within the spectral range of 0.75 – 6.5 eV, as functions of inverse grain radius R^{-1} with linear coefficients $h\nu_{gn}$ (h being Planck's constant and ν_{gn} being the group speed of excited electrons associated with the nth CP); (3) variations of the resonance energies E_n of CdTe films for all major critical points in the spectral range of 0.75 – 6.5 eV, as approximately linear functions of stress P in the film with stress coefficients C_P. In this report, we conclude our studies to deduce the above coefficients and the corresponding single crystal values for all the major critical points of both CdTe and CdS films. These coefficients along with the single crystal values form a comprehensive database that makes it possible to optically monitor film properties, such as temperature, grain structure and defects, as well as stress, on a solar cell production line at measurement high speed. As a first test of the potentialities, the database is used to analyze spectroscopic ellipsometry data taken during stepwise etching of a $CdCl_2$ treated CdTe solar cell. Depth profiles in the void volume fraction and electron mean free path are deduced that are qualitatively consistent with observations based on other techniques.

2.2 Review of Experimental Details

Polycrystalline CdTe and CdS films were magnetron sputtered under the conditions listed in Table 2. Native oxide-covered crystalline Si wafers were used as substrates due to their consistent smoothness. The deposition temperature T_s, a key process variable, was determined from the E_0 band gap shifts that occur upon cooling the deposited film to 15°C (the steady-state temperature of the substrate holder with cooling water flowing and heater off) and reheating to T_s. The ellipsometer used in this study provides ellipsometric spectra (ψ, Δ) over the range of 0.75 to 6.5 eV with 706 spectral points. The angle of incidence used in this study is ~65°. Each CdTe film was sputtered to a thickness of ~1000 Å; and each CdS film was sputtered to a thickness of ~500 Å, accurately determined from *in situ* real time spectroscopic ellipsometry (RTSE). For measurements versus temperature, the deposited film was stepwise cooled from T_s to 15°C under vacuum, during which *in situ* SE data were taken at each step of measurement temperature T_m. The temperature was calibrated from the E_0 band gap shifts as described previously. As a result, the optical properties of each CdTe and CdS film were obtained as a function of both T_s and T_m.

Table 2. Deposition parameters used in this study.

Deposited material	RF power (Watt)	Ar pressure (mTorr)	Ar flow (sccm)	Deposition temperature (°C)
CdTe	60	18	23	188-304
CdS	50	10	23	145-320

2.3 Review of the CdTe and CdS Dielectric Functions and Critical Points

Fig. 5 (a) shows the complex dielectric functions for two CdS samples. The E_0, E_1-A, and E_1-B critical points are evident. Fig. 5 (b) shows the complex dielectric functions for a set for two CdTe samples. In this case, the E_0, E_1, $E_1+\Delta_1$, and E_2 critical points are evident. To quantify these CPs, the second derivative spectra in ε were fit with the parabolic band approximation:

$$\varepsilon = \sum_n A_n (E - E_n - i\,\Gamma_n)^{\mu_n} \exp(i\phi_n) \qquad (1)$$

where A_n, E_n, Γ_n, μ_n, and ϕ_n are the amplitude, band gap (resonance energy), broadening parameter, exponent, and phase of the nth CP, respectively. A typical such fit is shown in Figure 6 for (a) CdS and (b) CdTe respectively.

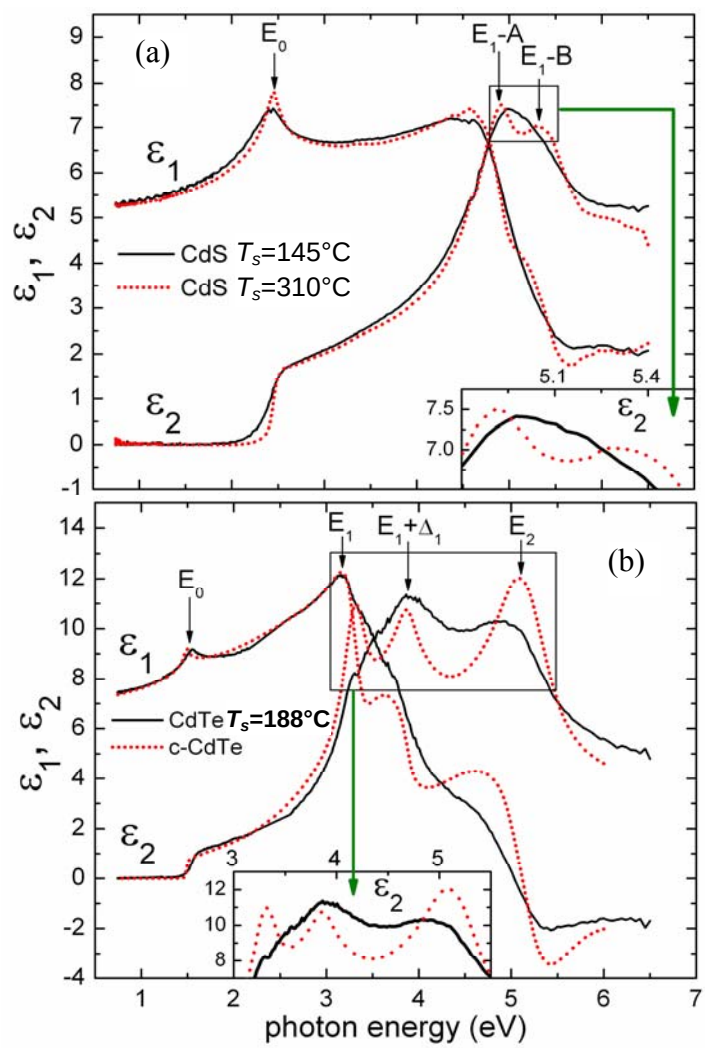

Figure 5. The T_m=15°C complex dielectric functions of: (a) two CdS samples deposited at 145°C and 310°C respectively; (b) single crystal CdTe and the CdTe film deposited at 188°C. Major critical points in this spectral range are marked with downward arrows (black).

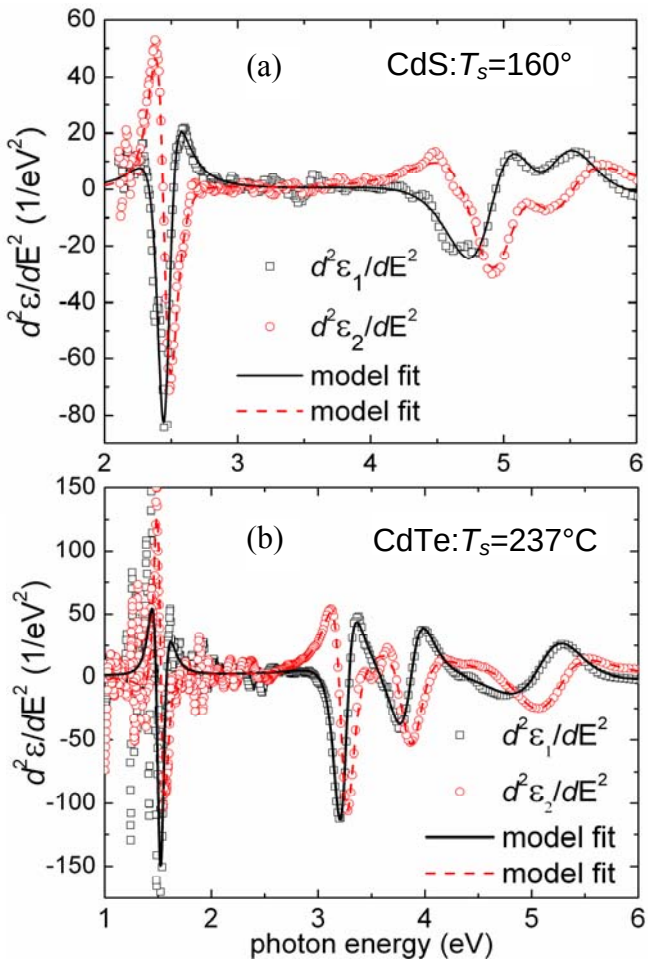

Figure 6. The 2nd derivative spectra of the T_m=15°C complex dielectric function of (a) the CdS film deposited at 160°C; and (b) the CdTe film deposited at 237°C. The model fits are based on Eq. (1).

2.4 Temperature Coefficients for Higher Energy CPs

Previously, we reported the variations of E_0 and Γ_0 of CdTe and CdS films with measurement temperature T_m. E_0 can be considered as an "independent" CP, while higher energy CPs are close to each other in energy and parameter correlation can easily occur (see Figs. 5 and 6). So fewer free parameters per CP were used for the higher energy CP parameters with T_m. As an example for CdS, Figure 7 shows that, similar to the E_0 CP, the higher energy CPs followed followed linear trends reasonably well for both the broadening parameters (upward slopes) and resonance energies (downward slopes). These results support the validity of the analyses. The temperature coefficients for both CdTe and CdS are indicated in the figures and summarized in Table 3.

2.5 Stress Coefficients

As reported previously, the sputtered CdS films have large amount of built in stress (deduced from the shift of the E_0 energy relative to single crystal CdS). If the E_1-A and E_1-B CP energies are assumed to vary linearly with deduced stress, as exemplified in Fig. 8 for E_1-A, then the stress coefficients can be determined. These coefficients are included in the summary of Table 3.

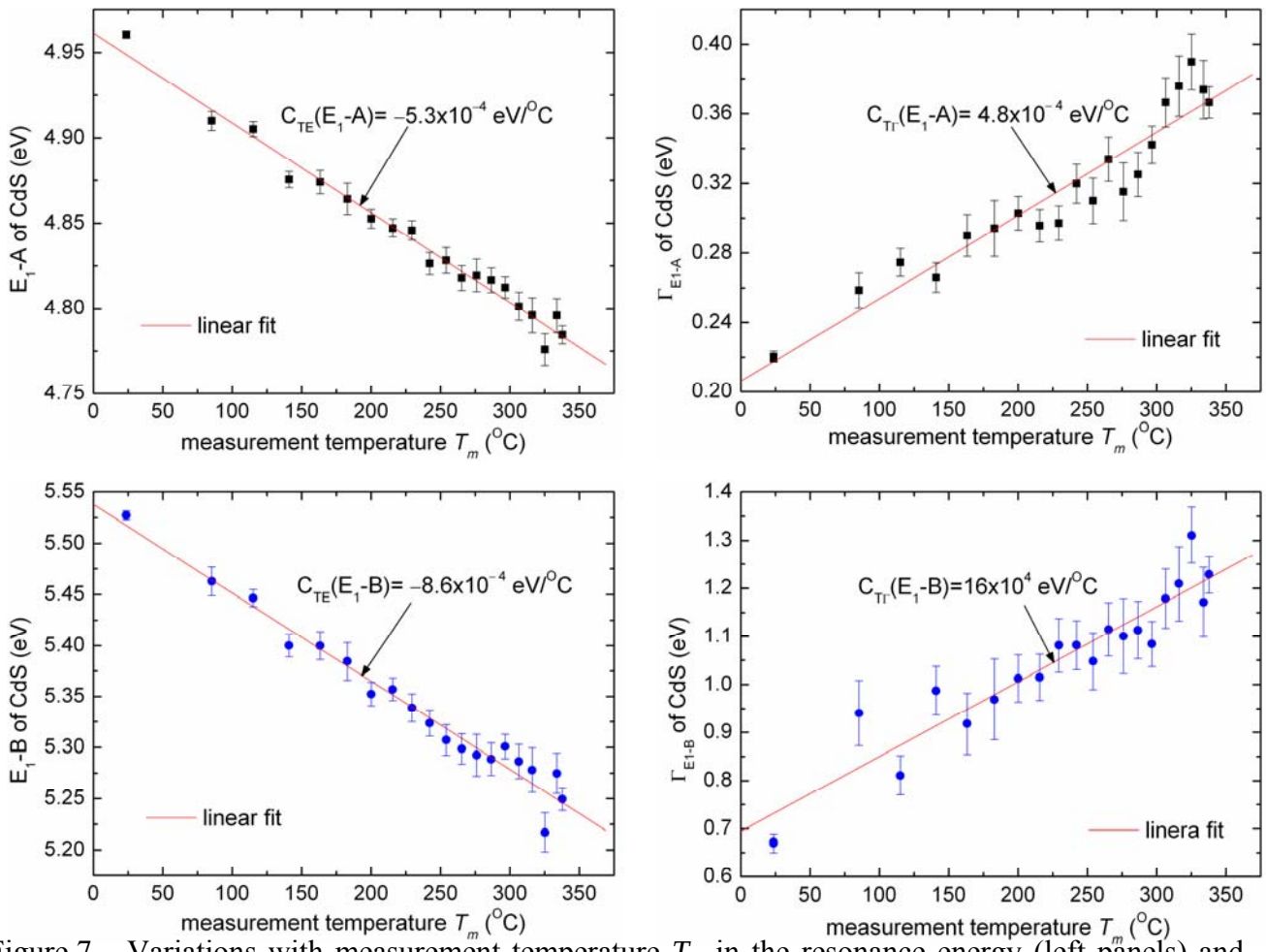

Figure 7. Variations with measurement temperature T_m in the resonance energy (left panels) and broadening parameter (right panels) of the E_1-A (upper panels) and E_1-B (lower panels) CPs of a CdS film. The indicated temperature coefficients are slopes of the linear fits.

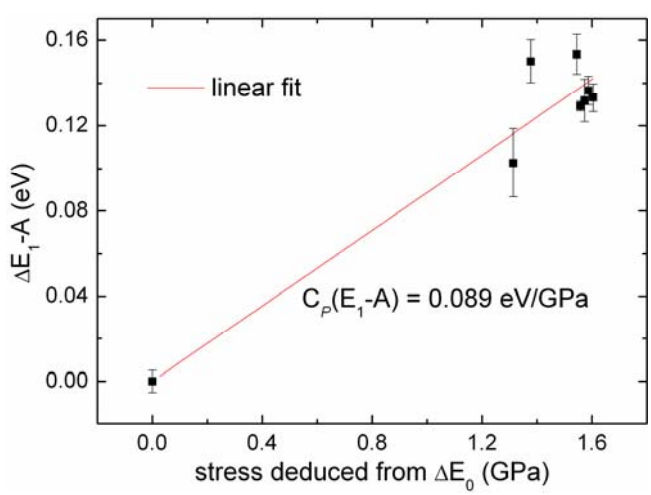

Figure 8. Shift in the T_m=15°C E_1-A CP energy of the CdS films relative to that of c-CdS, plotted vs. deduced stress. The linear fit is forced to pass (0, 0), representing single crystal CdS.

Table 3. Single crystal CP energies and widths, temperature coefficients of CP energies and widths, electron group speeds, and stress coefficients of CP energies for major CPs for CdTe and CdS.

CdS	$E_b(T_0)$ (eV)	$\Gamma_b(T_0)$ (eV)	$C_{T\Gamma}$ (eV/°C)	C_{TE} (eV/°C)	V_g (m/s)	C_P (eV/GPa)
E_0	2.38	0.071	2.0×10^{-4}	-4.1×10^{-4}	2.2×10^{5}	0.045
E_1-A	4.82	0.21	4.8×10^{-4}	-5.3×10^{-4}	3.3×10^{5}	0.089
E_1-B	5.50	0.64	16×10^{-4}	-8.6×10^{-4}	8.8×10^{5}	0.028
CdTe	$E_b(T_0)$ (eV)	$\Gamma_b(T_0)$ (eV)	$C_{T\Gamma}$ (eV/°C)	C_{TE} (eV/°C)	V_g (m/s)	C_P (eV/GPa)
E_0	1.49	0.041	1.2×10^{-4}	-3.7×10^{-4}	2.3×10^{5}	0.065
E_1	3.31	0.30	2.2×10^{-4}	-7.3×10^{-4}	8.1×10^{5}	-0.20
$E_1+\Delta_1$	3.89	0.29	5.1×10^{-4}	-2.5×10^{-4}	6.9×10^{5}	0.23
E_2	5.16	0.92	18×10^{-4}	-2.7×10^{-4}	4.2×10^{5}	0.16

2.5 Parameterization

Capabilities for on-line optical monitoring are being sought beyond simple thickness and compositional information described previously. The additional information that may be deduced includes grain size, stress, and temperature. These film characteristics have a significant influence on the critical point energies and/or widths and so should be determinable from fitting the optical spectra. Over the experimental ranges of this study, the effect of measurement temperature T_m, inverse mean free path R^{-1}, and stress P on the CP energies and widths can be well approximated by coupled linear dependences:

$$\Gamma = \Gamma_b(T_0) + C_{T\Gamma} * (T_m - T_0) + (hv_g/R)$$
$$E = E_b(T_0) + C_{TE} * (T_m - T_0) + C_P P \qquad (2)$$

where Γ_b and E_b are the width and CP energy of the single crystal (b: "bulk"); T_0 is a reference measurement temperature, normally room temperature; $C_{T\Gamma}$ and C_{TE} are the temperature coefficients of the CP width and CP energy, respectively; h is the Plank's constant; and v_g is the group speed of excited electrons; R is the excited electron mean free path, often the grain size in polycrystalline materials; C_P is the stress coefficient of the CP energy, and P is the stress. Equations (2) apply to all CPs for both CdTe and CdS. The corresponding coefficients and single crystal values are summarized in Table 3.

Because the complex dielectric function spectra ε of CdTe and CdS can be well parameterized with Eq. (1), including the CP energies and widths, then they can be further parameterized with Eqs. (2) as functions of the key sample characteristics of temperature, grain size, and stress. For a given layer, all the CPs share the same measurement temperature T_m, grain size R and stress P; furthermore, for a given solar cell, T_m for CdTe and CdS are the same. In addition, for a series of

cells of the same component materials (CdTe and CdS) but with different characteristics, the single crystal CP values, Γ_b and E_b, the CP coefficients, C_{TT} and C_{TE}, and the electron group speeds v_g, are all constants. As a result, not only can Eqs. (2) reflect interesting film characteristics, but also provide a useful "interlocking" mechanism that can significantly reduce correlation and drift in parameterization as often seen when only Eq. (1) is used.

2.6 Application

To demonstrate the parameterization described above, a $CdCl_2$-treated CdTe superstrate solar cell (without back contact) was stepwise chemically etched in a solution of 0.04 vol. % Br_2 in methanol. Depending on the length of etching time, each etch step removed from 100 to 1400 Å of CdTe. *Ex situ* spectroscopic ellipsometry data were collected after each etch. For better depth resolution, only those data in the spectral range of 3.7 to 6.0 eV were analyzed since the penetration depth in this range is no more than 200 Å. In this way, the complexity of the underlying CdS and TCO/glass layers was avoided in the optical model. Therefore, the model consists of: (1) a semi-infinite CdTe layer of temperature T_m, excited electron mean free path R, stress P, and void volume fraction f_v; (2) a surface roughness layer whose dielectric function is calculated with the Bruggeman effective medium theory assuming a 0.5/0.5 volume fraction mixture of CdTe and void.

In the range 3.7~6.0 eV, the CdTe dielectric function has 2 major CPs: $E_1+\Delta_1$ and E_2, which were modeled with Eqs. (1) and (2). Since the experiments were performed at room temperature, T_m was fixed at 25°C. This study and a previous one have shown that the stress effects on the CPs of $CdCl_2$ treated CdTe are negligible, so P was fixed at 0. Thus, the information of interest includes f_v and R. Fig. 9 shows a fit to ellipsometric (ψ, Δ) spectra that yields R=39.8±8 nm and f_v=0.038±0.004.

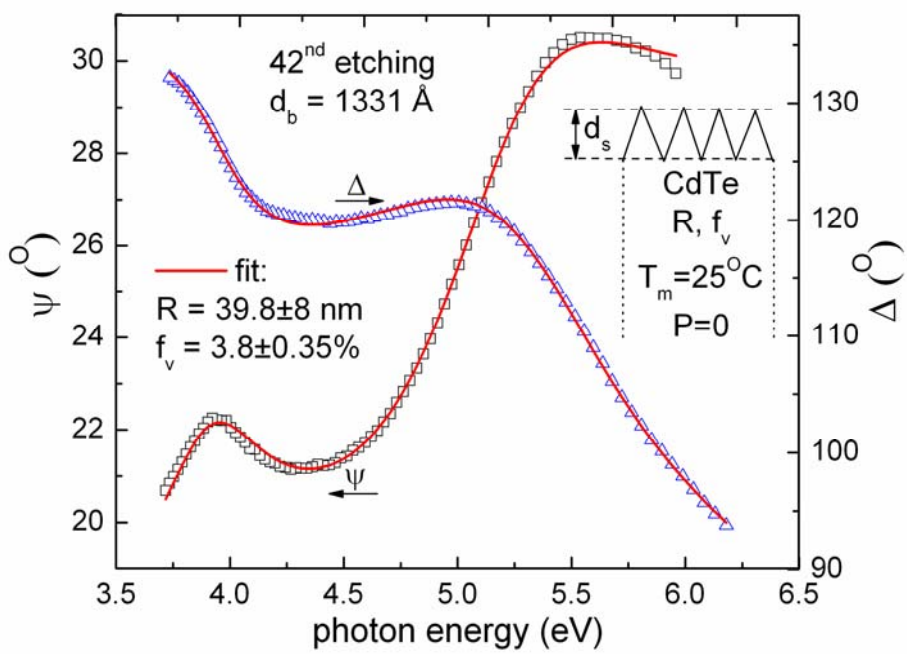

Figure 9. A typical fit to the ellipsometric spectra (ψ, Δ) in the analysis of stepwise etching data for a CdTe solar cell. The fit was performed to ψ and Δ simultaneously, based on the indicated optical model, and Eqs. (1) and (2) with CP parameters in Table 3.

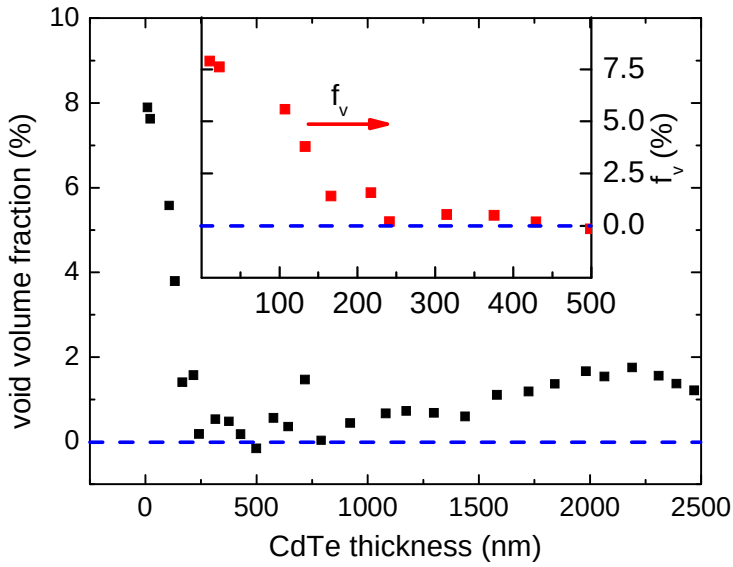

Figure 10. Void volume fraction depth profile in the CdTe layer of a $CdCl_2$ treated solar cell.

Figure 10 depicts the depth profile in f_v versus CdTe bulk layer thickness. The latter was determined from the ellipsometric data in the lower photon energy range with a more complicated optical model that includes all the layers of the solar cell structure. The rapid increase in f_v as the CdS/CdTe interface is approached may be attributed to lattice mismatch at the interface as well as to relaxation of stress after the $CdCl_2$ treatment. Figure 11 shows the mean free path depth profile, which can be roughly divided into 4 regions: (1) In the CdTe thickness range of 0~25 nm, an apparent sharp drop in *R* is observed as the CdTe thickness approaches 0. This can be attributed to S diffusion and alloying which enhances electron scattering. Thus, in this first regime, *R* may indicate the average distance between scattering centers in the alloy rather than an actual grain size; hence "effective grain size" is used in Fig. 8. In fact, a CdTe/CdS intermixed layer was also included in the model and was reduced by etching after the CdTe itself was etched away. This reduction is indicated by the negative values of thickness in the figure; (2) In the CdTe thickness range of 25~150 nm, the grain size is stabilized at ~40 nm with little increase. This may be an effect of lattice mismatch and void that suppresses the coalescence of grains during $CdCl_2$ treatment; (3) As the CdTe thickness increases above 150 nm, the grain size undergoes a steady increase and enters region (4) where the thickness is greater than ~300 nm and the grains are so large that the optical model cannot be used to distinguish between the polycrystalline film and single crystal CdTe. Both the void structure and the electron scattering near the CdTe/CdS interface are of interest due to their potential effects on solar cell performances.

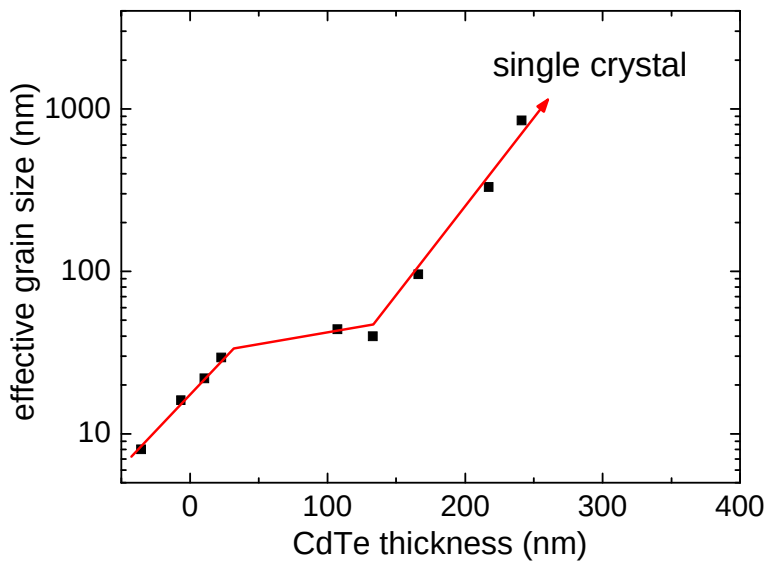

Figure 11. Effective grain size depth profile in the CdTe layer of a $CdCl_2$ treated solar cell. The negative thickness values represent the depth into the CdTe/CdS intermixed layer after all the pure CdTe layer was etched away.

2.6 Summary

RTSE has been applied to investigate the dielectric functions of CdTe and CdS thin films sputtered at different temperatures. These dielectric functions are modeled using the critical point (CP) parabolic band approximation. Key characteristics can be deduced including grain size, excitation group speeds, stress, and temperature from the CP parameters. Capabilities for on-line optical monitoring are sought to provide information, not only on layer thicknesses and compositions, but also on grain size, stress, and temperature. As a first application, the parameterization was used to analyze the ellipsometric spectra of a stepwise etched CdTe solar cell. In this study, depth profiles in the void and grain size near the CdTe/CdS interface have been obtained.